Analysis of Dislocation Density for GaN Based HEMTs in Screw Mod

Özlem BAYAL[1*] (iD) Esra BALCI[2] (iD) A. Kürşat BİLGİLİ[3] (iD) M. Kemal ÖZTÜRK[3] (iD) Süleyman ÖZÇELİK[4] (iD) Ekmel ÖZBAY[5] (iD)

[1]Photonics Application and Research Center, Gazi University, Ankara, Türkiye
[2]Department of Physics, Ankara Hacı Bayram Veli University, Ankara, Türkiye
[3]Department of Physics, Faculty of Science, Gazi University, Ankara, Türkiye
[4]Department of Photonics, Faculty of Science, Gazi University, Ankara, Türkiye
[5]NANOTAM, Bilkent University, Ankara, Türkiye

Keywords	Abstract
Screw Dislocation HEMT III-V Group Nitrur MOCVD HRXRD	Quick response is an important feature in design of optoelectronic cards. So, in this study, structural properties of GaN/AlN/AlGaN HEMTs structures grown on sapphire by the chemical vapor adjustment method are analyzed by the X-ray diffraction method. The main property of these kind of materials is that they are resistant to high voltage, temperature, and pressure. Although their performance is worse compared silicon, for forcing limit standards, they present wide research field. In this study, the focus of investigation is dislocation density stemming from lattice mismatch between layers and wafer causing cracks on the surface. In HEMT structure calculation of dislocation density for GaN and AlN represents all structure. High dislocation density for AlN layer is determined because of aggressive behavior of Al element in the structure. Also, quantized GaN layers stop moving of dislocations and prevents surface cracks.

Cite

Author ID (ORCID Number)		Article Process	
0000-0003-0718-9734	Özlem BAYAL	**Submission Date**	06.12.2022
0000-0003-0217-9481	Esra BALCI	**Revision Date**	23.01.2023
0000-0003-3420-4936	Ahmet Kürşat BİLGİLİ	**Accepted Date**	21.02.2023
0000-0002-8508-5714	Mustafa Kemal ÖZTÜRK	**Published Date**	22.05.2023
0000-0002-3761-3711	Süleyman ÖZÇELİK		
0000-0003-2953-1828	Ekmel ÖZBAY		

1. INTRODUCTION

Today, III-V group semiconductor nitrites such as AlN, GaN and AlGaN and their alloys forms the base of electronic and opto-electronic devices as light emitting diodes (LED), laser diodes, UV sensors and high electron mobility transistors (HEMT) because of their physical properties (Kapolnek et al., 1995; Heinke et al., 2000). These semiconductor nitrites and their alloys crystallize both in wurtzite and zinc-blende structures (Strite & Morkoç, 1992; Vurgaftman et al., 2001). The basic difference between these two structures is the rank of planes. Wurtzite structure is regulated as triangle (0001) tighly packed planes. Zincblende structure is formed as tighly packed atoms in (111) plane as triangles along <111> direction. III-V group semiconductor nitrites have direct and wide band gaps. In semiconductors with direct band gap, recombination of electrons and holes comes out in δk=0 without a change in momentum. This situation implies III-V group semiconductor nitrites that are effective for photon producers (Chen et al., 2020). At the same time, mobility increases if conduction conditions are maintained because of direct band transition. Band gaps of III-V group semiconductor nitrites are 0.7, 3.4, and 6.1 eVs for InN, GaN and AlN respectively (Elhamri et al., 1998). Because working principle of electronic and opto-electronic devices are dependent on physical properties of materials forming the device. Direct band transition feature gives hand to many different applications in a wide wavelength range (Wu et al., 2002). For instance, in billboards, traffic lamps or cell phones using nitrite based HEMTs, maintains many advantages in terms of power depletion, cost and efficiency. On the other hand,

*Corresponding Author, e-mail: ozlembayal@gmail.com

nitrites can operate at high temperatures with low noise because of their good thermal conductivity. Also, III-V group nitrites have the property of well electron carrying, good mobility value and saturation speed. These features enable GaN based HEMTs to be used in radars, rockets and satellite systems those require high temperature and high power (Bayrak, 2003). III group nitrites are also convenient for quantum wells, modulation doped hetero interfaces, heterojunction structures and hetero structure technology (Morkoç, 1999).

Because of difficulties in growth of GaN crystal, GaN/AlGaN heterojunction structures are grown on sapphire (Al_2O_3) wafers despite there is low thermal and structural match (Kapolnek et al., 1995). The reason of choosing sapphire is its hexagonal symmetry, easy handling, easy cleaning procedure before growth and low cost. Also, melting point of sapphire is 2040ºC and this property makes it chemically stable at even very high temperatures. But sapphire is not an ideal wafer for commercial applications. The reason for this is high dislocation density stemming from great lattice mismatch between sapphire and III-V group nitrites and mismatch between thermal expansion coefficients. Lattice mismatch is about 14-16% and thermal expansion coefficient mismatch is about 34% (Bernardini et al., 1997).

In this study, structural properties and mosaic defects of AlN/GaN/AlGaN structure are investigated on three different samples. It is seen that gained data and analysis concluded with great accordance with literature. Investigation of this type of samples are rare in literature, so this study may play a key role for researchers for their future studies. The defect nature of these structures is predominantly attributed to the dislocation density. Finding the dislocation in monolayer structures is easy (Feaugas & Delafosse, 2019). Although finding the dislocation density of interfaces in a multi-quantum HEMT structure sheds light on an important problem. In this study, we aim to find the defect factors and increase the quality of the HEMT structure.

2. MATERIAL AND METHOD

GaN/AlN/AlGaN HEMT samples were grown on sapphire wafer by the MOCVD technique. Al pre-deposition did not applied and the growth process can be summarized as follows. Surfaces were clean and mirror like, there were colourful crowding fields on the surface. GaN thin film is deposited on 520 nm thick AlN layer Over this GaN buffer layer 2 nm thick AlN inter layer is grown. Later 25 nm thick AlGaN layer is grown on AlN inter layer. AlGaN layer is grown at 1075°C -1140°C temperature range under NH_3 flow and 50 mbar medium pressure 3 nm thick GaN cap layer is grown at the last step of sample growth.

Deposition is made at 1050°C for 15 minutes. During preparation of samples sapphire is used as a wafer. To construct high electron mobility transistor (HEMT), AlGaN layer is deposited on AlN nucleation layer in MOCVD. This structure is grown as stable as possible. Five layers of quantized GaN layers are used to prevent or reduce dislocations. Schematic diagram of samples is shown in Figure 1. in experimental section. To prevent dislocations stemming from lattice mismatch between sapphire and GaN buffer layer AlN nucleation layer and AlN buffer layers are grown at high temperature. AlN inter layer is grown in 1075°C and 1140°C temperature range with triethylaluminium TMAl sources under NH_3 flow with flow speed of 200 sccm and 10 sccm respectively under 50 mbar pressure in a duration of 3 minutes. Nucleation layer is grown at 550-560°C temperature that ranges under 50 mbar pressure with NH_3 flow at speed of 1000 sccm and TMAl source with flow speed of 15 sccm.

In the expectation that GaN/AlGaN HEMT structures in detail, High Resolution X-Ray Diffraction (HRXRD), noncontact Hall measurement, and Atomic Force Microscopy (AFM) (Nanomagnetic Instruments) in dynamic mode scanning measurement were examined in this study.

XRD analysis is made with Bruker D-8 discovery HRXRD diffractometer. This device uses X- rays with a wavelength of 0.54056 nm with pure $CuK\alpha_1$ source and four channel Ge monochromator. Scans for samples are made on (101), (102), (103), (105), (106), (112), (114), (121), (122), (123), (124), (201), (202), (203), (204), (211), (212), (213), (301), (302) symmetric and asymmetric planes. These plane scans are made for AlGaN, AlN and GaN individually. The surface morphology of samples was characterized by Atomic Force Microscopy (AFM) (Nanomagnetic Instruments) in dynamic mode scanning.

Figure 1. *The schematic diagrams of samples*

3. RESULTS AND DISCUSSION

In defected epilayers, FWHM of ω curves are formed by support of tilt, twist, mean size of grains and in-homogeneous stress and strain dispersion. In principle expansion may be important because of limited field dimension and strain but in present system it is determined that it has a little effect. Here to reduce or prevent expansion stemming from inhomogeneous strain and limited grain dimension, a slit with a 0.5 mm width is inserted in front of detector during use of double axis w scans. Also, samples present 10"-30" FWHM both with triple axis 2 theta scans and non-zero hk orientation in (00.2) reflection. Moreover, for all experimental reflections both inward expansion of crystal reflection and expansion stemming from device can be neglected. Because these effects take only a few arc seconds. Expansion caused by twist angle can be analyzed using reflections in screw geometry.

Nitrite materials are well-known with their cubic hexagonal structure. Nano structures has many advantages for opto-electronic devices in terms of optical and electrical properties. Nitrite materials have the advantage of operating at high voltage, temperature, and frequency. For instance, nitrite-made transformators can operate for a long time without getting out of order (Yang et al., 2022). In space works, these materials resist to high temperature very well and maintains operation of device for a long time. The reasons for this situation are point, line and volume defects spreading all over the structure. There are some methods to reduce these defects. In samples five layers of GaN are used to reduce defects. Tilt twist, grain size and dislocations can be given as examples of defects supporting broadening of FWHM. Broadening of FWHM stemming from device is enough to determine twist angle in screw geometry. In this situation grain size at some arc seconds dimension and inhomogeneous strain may be neglected and this makes calculation of twist angle, screw, and edge type dislocations available.

Sapphire is used as a wafer. Lattice mismatch between this layer and GaN is caused by clean mirror-like image of surface. Three samples are grown to examine defect properties by changing thickness of GaN layers and buffer AlN layer (Kato et al., 2021). Defect structure is examined in electrical, optical, and structural terms. To examine HEMTs, especially mobility is important gained by Hall device.

Figure 2 shows Φ scan of samples. Curves belonging to different samples are shown with different colors. Φ scan angles show optimized Φ angle value for Φ scan of planes. Because there is diffraction at every edge of hexagonal structure in Φ scan, there are six peaks between 60° and 360° range. Φ scan gives right value in pdf card for high quality GaN because Φ scan is optimized. For cubic systems there are four different peaks in Φ scan. Peak is optimized for Φ scan (Nand et al., 2022).

Figure 3. shows increasing FWHM for ksi Φ and ω scans for three samples. FWHM of Φ and ω scans are gained by using pseudo-voigt function from rocking curves. FWHM of a scan in Figure 3. decrease with an increase in ksi. On the other hand, (12.1) reflections approach each other because they are 78.8° in percentage. In fact, they should be equal when ksi angle reaches 90°. Diffraction geometry is shown in Figure 4. With the
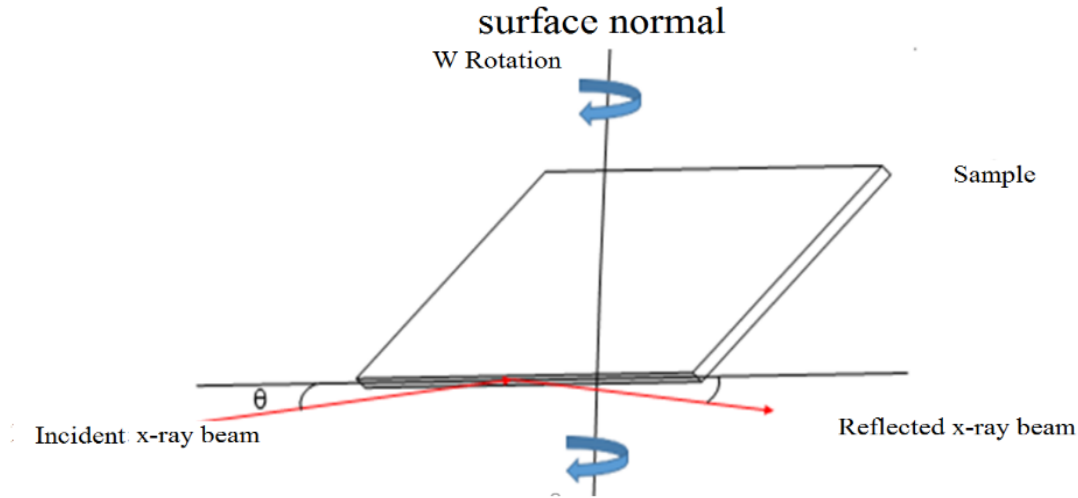
cause of too thin films reflection is impossible in 90° lattice plane tilt. Here it can be seen that in wurtzite structure and on (12.1) plane there are 12 similar planes.
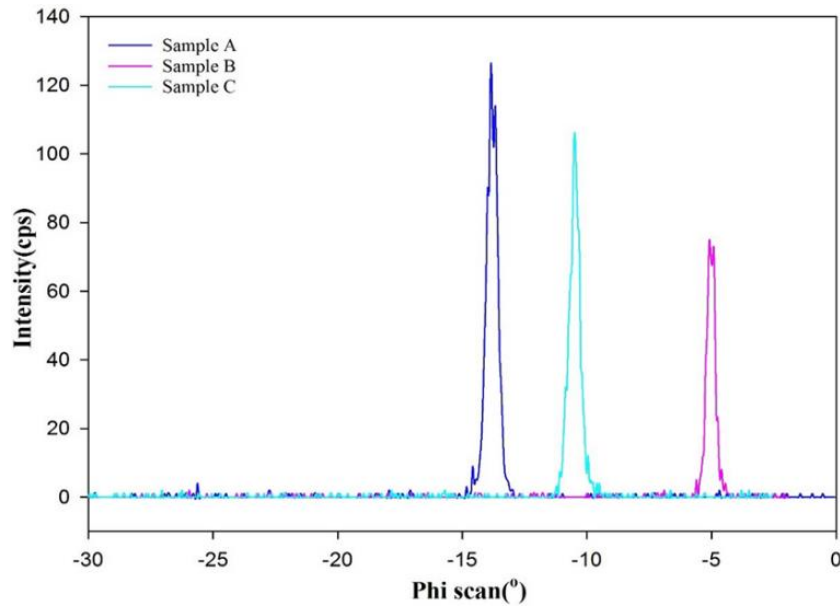
Figure 2. Φ scan of crystal planes for samples A, B and C
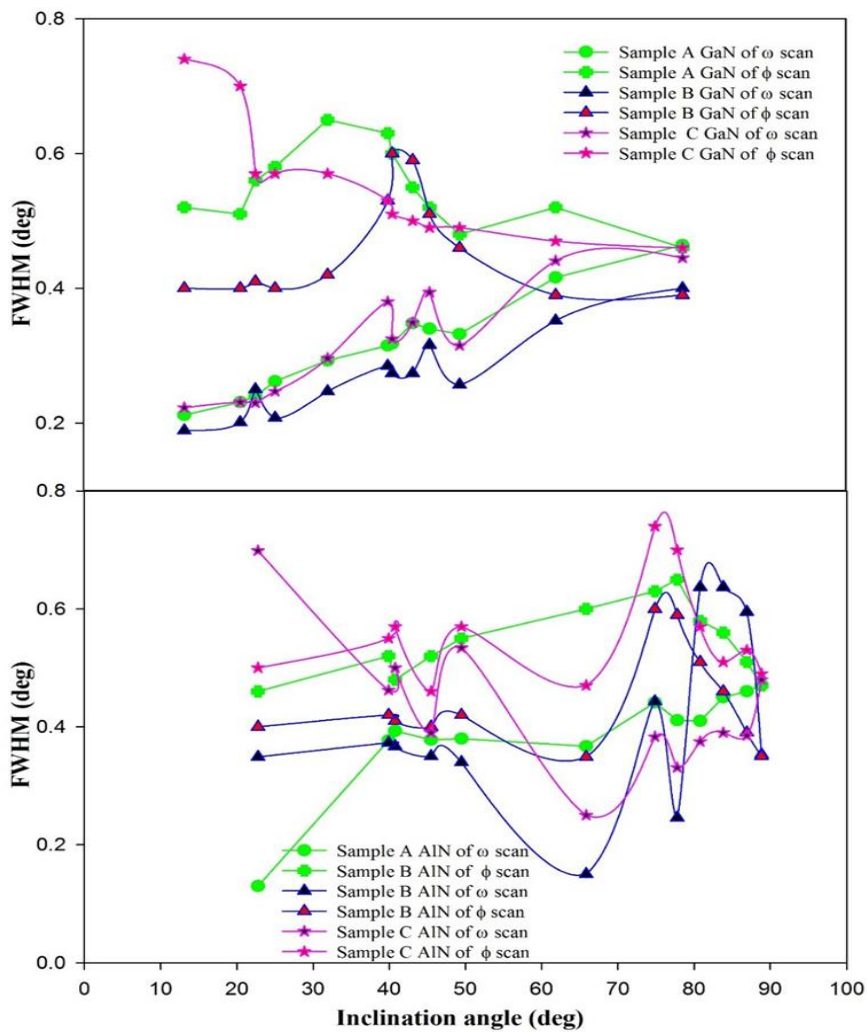
Figure 3. Φ and ω scans for GaN and AlN films in three samples

Figure 4. Screw dislocation of HEMT on HRXRD

Reflection peaks do not iterate at each 30° azimuth angle. Group six peaks iterate at every 60° azimuth angle and other groups behave similar but FWHM values of Φ and ω scans are equal. Although lattice have different hexagonal crystal structure on (12.1) diffraction plane twist angles are different for GaN and AlN layers. Quantized growth reduced dislocations. In addition, on tilt angle which the reflection is seen (78.8°) FWHM of Φ and ω scans are almost the same. These results imply width of rocking curves approach twist angle in Φ and ω scans at higher ksi angles. Also, difference in FWHM of scans are larger than ksi scans. For this reason, mean twist angle should be between FWHM and ksi=78.8°. In this situation, average value of FWHM and ksi=78.8° can be taken as mean twist angle.

In order to test validity of results, when compared with Srikant and co-workers' method, it is seen that they correspond each other (Heinke et al., 2000). Appear to be compatible with each other. Little difference between twist angle calculated in this study and twist angle value in literature can be calculated as ±0.005° . This result is in borders of instrumental resolution. To determine twist angle of different defected structures is also possible with this method.

To compare GaN and AlN on (002) plane rocking curves are given in Figure 5. While GaN layers are in a uniform width position AlN is fluctuating with a strain value. This means that for all three samples (002) plane is crystallized and (002) orientations are in texture structure. On (004) plane there are differences in crystallite GaN structures. For AlN GaN in sample A there is low peak intensity but high FWHM. On these planes GaN lattice match is seen and AlN strain fluctuations are expanded. On (006) plane GaN layer is well crystallized and for sample A AlN is extremely fluctuated with strain.

As can be seen in Table 1 twist angles increase with a decrease in tilt angles. Estimated dislocation density values can be calculated with Equations (1), (2) and (3).

$$D_{screw} = \frac{\beta^2_{(00.2)}}{9b^2_{screw}} \tag{1}$$

$$D_{edge} = \frac{\beta^2_{(12.1)}}{9b^2_{edge}} \tag{2}$$

$$D_{dis} = D_{screw} + D_{edge} \tag{3}$$

Beta is FWHM of rocking curves and *b* screw and edge are the length of burgers vector. As known before, twist range of lattice planes for wurtzite GaN films uses burgers vector b= [001] and screw type dislocations (Gay et al., 1953; Look & Sizelove, 1999). Tilt range of lattice plane shows details of burgers vector and edge type dislocation density. Number of samples versus dislocation density plot is shown in Figure 6. Dislocation densities of GaN films are too different from each other. It is still being investigated how these dislocations effect electrical and optical features of device.
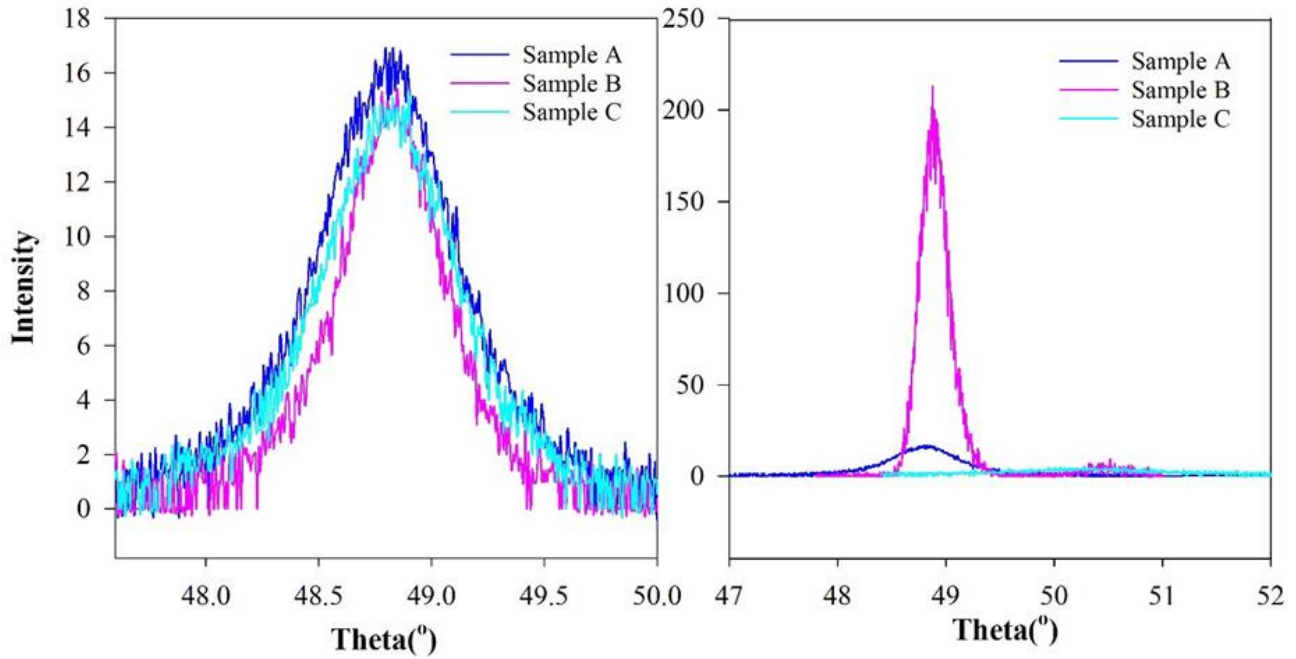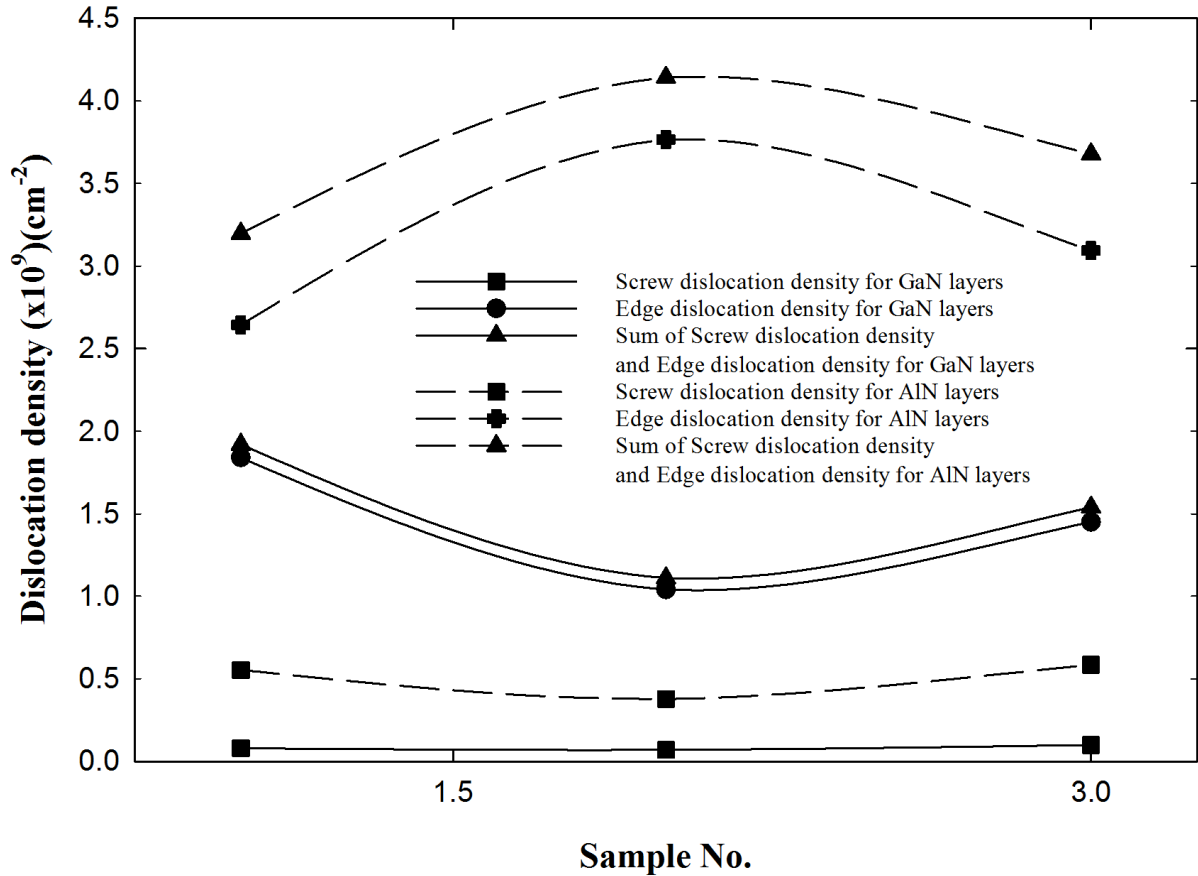

Figure 5. HRXRD omega curves of (002) miller plane of GaN and AlN layers in HEMT structures.

Table 1. GaN films are the rocking curves of Φ and ω scans of experimental results

Samples		Measurement results			
		FWHM (deg)			
		(00.2) reflection	ω scan of (12.1) reflection	Φ scan of (12.1) reflection	Twist angle with error correction (deg)
GaN	A	0.08	0.28	052	0.54
	B	0.07	0.20	0.46	0.43
	C	0.09	0.21	0.57	0.49
AlN	A	0.21	0.235	0.41	0.44
	B	0.17	0.175	0.34	0.35
	C	0.22	0.305	0.62	0.62

Özlem BAYAL, Esra BALCI, A. Kürşat BİLGİLİ, M. Kemal ÖZTÜRK, Süleyman ÖZÇELİK, Ekmel ÖZBAY

Figure 6. *Presentation of calculated screw and edge type dislocations*

Twist angle of AlN is larger than other layers. Fluctuations in samples show that there is no linear behavior. It can clearly be seen that defect structure difference is large for AlN/GaN crystallite size. Al dislocations show screw and edge dislocations. It is higher than the GaN dislocation value. Because AlN is an aggressive material, there is a mismatch incompatibility with GaN.

It is clearly seen in Figure 7, for sample A the exposed AlN surface is smooth with the surface roughness of 2.14 nm. sharp rocky mountain-like morphological structure but macro grain crystal structures are observed in sample A. In sample B with a lot of grain and high roughness. Sample B with the rms value is 1.00 nm has more smooth surface than Sample A. The sample C which has moderate grain structures with rms value is 4.21 nm. Dielectric layer between metal and semiconductor converts metal-semiconductor (MS) structure to metal insulator semiconductor (MIS) structure. The interface layer with increasing thickness is in equilibrium with the semiconductor. (Bilgili et al., 2022)
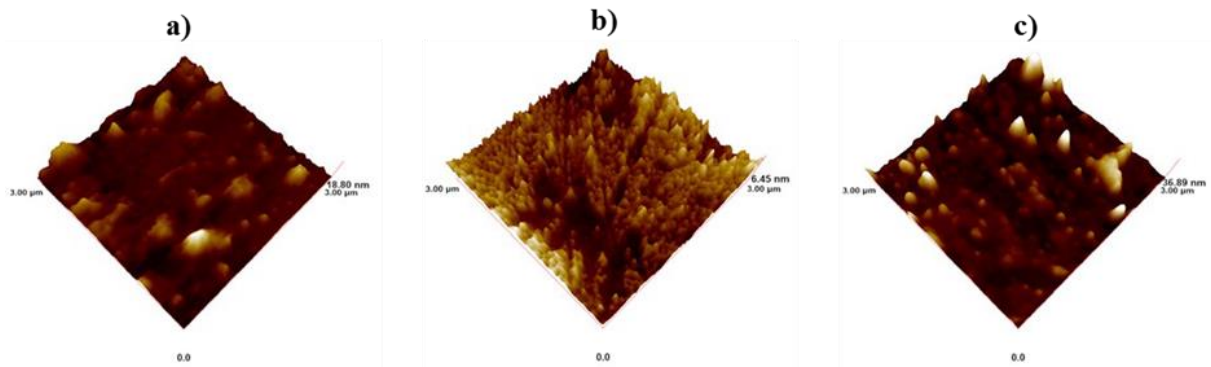
Figure 7. *AFM images of a) sample A, b) sample B and c) sample C*

4. CONCLUSION

HRXRD makes investigation of line defects for inter-layers available for HEMT structure with this method. Defect reduction of optoelectronic devices plays an important role in improving the performance of crystal structure properties in IV characterization of mobility movements. In addition to being stable at high voltage current frequency values, HEMTs LEDs Diodes door switches with effective selectable wavelengths provide advantages in many optoelectronic devices (Subramanian et al., 2020). For this purpose, defect analysis in HEMT structure was analyzed with HRXRD with weighted dislocation density. According to the analysis result, AlN and GaN dislocation densities were calculated with high precision according to the surface and interface densities. Both AlN and GaN dislocation densities showed similar type properties in the increasing sample. AlN defect structures of these structures are gradually seen in GaN. We see that this harmony remains within the dislocation of the GaN wafer layers, which is about $4 \times 10^9 \text{cm}^{-1}$. Dislocation densities are compatible with the amplification mobility of our sample.

Data availability statement: All data used in this work are available from the author.

Author contributions: Özlem Bayal, wrote the manuscript, Esra Balcı, made the measurements, made the calculations, Mustafa Kemal Öztürk, Süleyman Özçelik, Ekmel Özbay maintained device support.

CONFLICT OF INTEREST

The authors declare no conflict of interest.

REFERENCES

Bayrak, S. T. (2003) *AlxGa1-xN/GaN hetero yapılardaki 2BEG'nın elektriksel ve optiksel karakterizasyonu* MSc Thesis, Balıkesir University.

Bernardini, F., Fiorentini, V., & Vanderbilt, D. (1997). Spontaneous polarization and piezoelectric constants of III-V nitrides *Physical Review B*, *56*(16), R10024. doi:10.1103/PhysRevB.56.R10024

Bilgili, A. K., Çağatay, R., Öztürk, M. K., & Özer, M. (2022). Investigation of Electrical and Structural Properties of Ag/TiO$_2$/n-InP/Au Schottky Diodes with Different Thickness TiO$_2$ Interface. *Silicon*, *14*(6), 3013-3018. doi:10.1007/s12633-021-01093-5

Chen, Y., Liu, J., Zeng, M., Lu, F., Lv, T., Chang, Y., Lan, H., Wei, B., Sun, R., Gao, J., Wang, Z., & Fu, L. (2020). Universal growth of ultra-thin III–V semiconductor single crystals. *Nature Communications*, *11*(1), 3979. doi: 10.1038/s41467-020-17693-5

Elhamri, S., Newrock, R. S., Mast, D. B., Ahoujja, M., Mitchel, W. C., Redwing J. M., Tischler, M. A., & Flynn, J. S. (1998). Al$_{0.15}$Ga$_{0.85}$N/GaN heterostructures: Effective mass and scattering times. *Physical Review B*, *57*(3), 1374-1377. doi:10.1103/PhysRevB.57.1374

Feaugas, X., & Delafosse, D. (2019). Hydrogen and crystal defects interactions: Effects on plasticity and fracture. In: C. Blanc, & I. Aubert (Eds.), *Mechanics - Microstructure - Corrosion Coupling Concepts, Experiments, Modeling and Cases* (pp. 199-222). Elsevier. doi:10.1016/B978-1-78548-309-7.50009-0

Gay, P., Hirsch, P. B., & Kelly, A. (1953). The estimation of dislocation densities in metals from X-ray data. *Acta Metallurgica*, *315*(3), 315-319. doi:10.1016/0001-6160(53)90106-0

Heinke, H., Kirchner, V., Einfeldt, S., & Hommel, D. (2000). X-ray diffraction analysis of the defect structure in epitaxial GaN. *Applied Physics Letters*, *77*(14), 2145-2147. doi:10.1063/1.1314877

Kapolnek, D., Wu, X. H., Heying, B., Keller, S., Keller, B. P., Mishra, U. K., DenBaars, S. P., & Speck, J. S. (1995). Structural evolution in epitaxial metalorganic chemical vapor deposition grown GaN films on sapphire. *Applied Physics Letters*, *67*(11), 1541-1543. doi:10.1063/1.114486

Kato, M., Asada, T., Maeda, T., Ito, K., Tomita, K., Narita, T., & Kachi, T. (2021). Contribution of the carbon-originated hole trap to slow decays of photoluminescence and photoconductivity in homoepitaxial n-type GaN layers. *Journal of Applied* Physics, *129*(11), 115701. doi:10.1063/5.0041287

Look, D. C., & Sizelove, J. R. (1999). Dislocation Scattering in GaN. *Physical Review Letters*, *82*(6), 1237-1240. doi:10.1103/PhysRevLett.82.1237

Morkoç, H. (1999). General Properties of Nitrides. In: *Nitride Semiconductors and Devices* (pp. 8-44), (Springer Series in Materials Science, 32). Springer. doi:10.1007/978-3-642-58562-3_2

Nand, M., Tripathi, S., Rajput, P., Kumar, M., Kumar, Y., Mandal, S. K., Urkude, R., Gupta, M., Dawar, A., Ojha, S., Rai, S. K., & Jha, S. N. (2022). Different polymorphs of Y doped HfO2 epitaxial thin films: Insights into structural, electronic and optical properties. *Journal of Alloys and Compounds*, *928*, 167099. doi:10.1016/j.jallcom.2022.167099

Strite, S., & Morkoç, H. (1992). Microelectronics and Nanometer Structures Processing, Measurement, and Phenomena. *Journal of Vacuum Science & Technology B*, *10*(4), 1237-1266. doi: 10.1116/1.585897

Subramanian, B., Anandan, M., Veerappan, S., Panneerselvam, M., Wasim, M., Radhakrishnan, S. K., Pechimuthu, P., Verma, Y. K., Vivekanandhan, S. N., & Raju, E. (2020). Switching transient analysis and characterization of an E-mode B-doped GaN-capped AlGaN DH-HEMT with a freewheeling Schottky barrier diode (SBD). *Journal of Electronic Materials*, *49*(7), 4091-4099. doi:10.1007/s11664-020-08113-x

Vurgaftman, I., Meyer, J. R., & Ram-Mohan, L. R (2001). Band parameters for III–V compound semiconductors and their alloys. *Journal of Applied Physics*, *89*(11), 5815-5875. doi:10.1063/1.1368156

Wu, J., Walukiewicz, W., Shan, W., Yu, K. M., Ager III, J. W., Haller, E. E., Lu, H., & Schaff, W. J. (2002). Effects of the narrow band gap on the properties of InN. *Physical Review B*, *66*(20), 201403. doi:10.1103/PhysRevB.66.201403

Yang, Z., Zhong, Y., Zhou, X., Zhang, W., Yin, Y., Fang, W., & Xue, H. (2022). Metal-organic framework-based sensors for nitrite detection: a short review. *Journal of Food Measurement and Characterization*, *16*(2), 1572-1582. doi: 10.1007/s11694-021-01270-5